

# We are IntechOpen, the world's leading publisher of Open Access books Built by scientists, for scientists

**4,800**

Open access books available

**122,000**

International authors and editors

**135M**

Downloads

Our authors are among the

**154**

Countries delivered to

**TOP 1%**

most cited scientists

**12.2%**

Contributors from top 500 universities



**WEB OF SCIENCE™**

Selection of our books indexed in the Book Citation Index  
in Web of Science™ Core Collection (BKCI)

Interested in publishing with us?  
Contact [book.department@intechopen.com](mailto:book.department@intechopen.com)

Numbers displayed above are based on latest data collected.

For more information visit [www.intechopen.com](http://www.intechopen.com)



# Dynamic Viscosity of Graphene- and Ferrous Oxide-Based Nanofluids: Modeling and Experiment

*Majid Al-Wadhahi, G. Reza Vakili-Nezhaad  
and Ohoud Al Ghafri*

## Abstract

This study focused on measuring the viscosity and analyzing the behavior of two types of nanofluids: ferrous oxide-deionized (DI) water nanofluids and graphene-DI water nanofluids at different temperatures and volume fractions. Zeta potential measurement, which was performed to check the stability of the nanofluids, showed stable suspensions. All viscosity measurements were conducted using a capillary viscometer at temperatures ranging between 25 and 65°C. Both types of nanofluids showed increasing viscosity with increasing nanoparticle loading and decreasing viscosity with increasing temperature. Furthermore, experiments on different-sized ferrous oxide-based nanofluids revealed inverse relation between the size of nanoparticles and viscosity. An accurate model was developed based on the Buckingham Pi theorem to fit all factors affecting viscosity in a dimensionless form. These factors are the viscosity of the base fluid, nanoparticles' volume fraction, nanoparticles' size, the temperature of the system, some molecular properties, and zeta potential.

**Keywords:** nanofluids, dynamic viscosity, Buckingham Pi theorem, correlation, zeta potential

## 1. Introduction

Nanofluids have found many applications in science and industry. Because of the very complex nature of such fluids, the prediction of their thermophysical properties has become a challenging problem for research. Among these properties, viscosity has a vital role in all nanofluids' transport phenomena. Therefore, a great deal of effort has been made in the last two decades for developing reliable models to predict the viscosity of nanofluids. Some studies on nanofluids' rheological behavior were devoted to understanding whether these fluids are Newtonian or non-Newtonian toward finding their viscosity based on the relation between the shear stress and the shear rate. However, in fact, there are many factors affecting viscosity of nanofluids, such as temperature, pH, volume fraction, particles' size, particle size distribution, electrical double layer (EDL), zeta potential, base fluid

type, aspect ratio of particles, packing coefficient, particles' agglomeration, nanolayers, and magnetic properties for ferromagnetic type of nanoparticles. In the following, the most recent well-known models for estimating the viscosity of nanofluids will be summarized. Their application for our experimental data set will be elaborated. Then, a summary of the experimental works in the literature followed by our experiments will be presented. Finally, we will discuss the newly developed model and its performance with regard to the generated data set in the present chapter.

## 2. Theoretical models on viscosity of nanofluids

Classical models have predated the invention of the nanofluids, and they were on the rheological behavior of micrometer- or millimeter-sized suspensions. Nanofluids are solid-liquid binary fluids; however, they are closer to the fluid state, unlike conventional fluid containing micrometer- or millimeter-sized particles. Therefore, most classical theoretical models such as those developed by Einstein, Smoluchowski, Booth, Ward and Whitmore, Vand, Moony, Roscoe, Brinkman, Williams, Krieger and Dougherty, Frankel and Acrivos, Farris, Nielsen, Lundgren, Batchelor, Kitano, Graham, and others are inconvenient to estimate the viscosity of nanofluids, and we are not going to review them. Since our focus here is only on the viscosity of nanofluids, we will just present those models that have been developed for nanofluids. Therefore, the models proposed by Chen, Masoumi, Hosseini, Selvakumar, Dhinakaran, and White are presented in the following in brief.

In 2007, Chen et al. [37] modified the work of Krieger and Dougherty. They assumed a suspension of polydisperse particles (different sized particles), containing agglomerates, and therefore they derived a new correlation by introducing maximum packing fraction of agglomerates ( $\Phi_{ma}$ ) and the fractal index of agglomerates. This model is given by Eq. (1) where  $\Phi_a$  is given by ( $\Phi_a = \Phi/\Phi_{ma}$ ). The viscosity was assumed to follow a power law with a fractal index ( $D$ ). Thus,  $\Phi_a$  becomes  $[\Phi_a = \Phi(a_a/a)^{3-D}]$ , where ( $a_a/a$ ) is the ratio of effective radii of aggregates and primary nanoparticles.

$$\mu_{nf}/\mu_{bf} = \left(1 - \left(\frac{\Phi_a}{\Phi_m}\right)\right)^{-[\eta]\Phi_m} \quad (1)$$

In 2009, Masoumi et al. [39] developed a new semiempirical model, in which the effects of nanoparticle's density, Brownian motion, and some physical properties of the base fluid were considered. They analyzed the dispersion of nanoparticles in a fluid medium as a two-phase problem and considered five parameters affecting the viscosity of nanofluids, which are temperature, volume fraction, particles' size, nanoparticles' density, and the physical properties of the base fluid. Eqs. (2)–(4) show the proposed model with four empirical constants  $c_1$ ,  $c_2$ ,  $c_3$ , and  $c_4$ .

$$\mu_{nf} = \mu_0 + \frac{\rho_p v_B d_p^2}{72C\delta} \quad (2)$$

$$\delta = 3\sqrt{\frac{\pi}{6\phi}} d_p \quad (3)$$

$$C = \mu_0^{-1}[(c_1 d_p + c_2)\phi + (c_3 d_p + c_4)] \quad (4)$$

In 2010, Hosseini et al. [38] proposed a new semiempirical dimensionless model for the viscosity of nanofluids. They formulated their equation of relative viscosity based on four dimensionless groups, which consider the effect of the viscosity of the base fluid, volume fraction of nanoparticles, size of the nanoparticles, thickness of the capping layer, and temperature on the viscosity of the nanofluid. This model is given by Eq. (5), in which,  $\pi_1 = \frac{\mu_{nf}}{\mu_{bf}}$ ,  $\pi_2 = \Phi_i$ ,  $\pi_3 = \frac{d}{1+r}$ , and  $\pi_4 = \frac{T}{T_0}$ .

$$\pi_1 = \exp(m + \omega \pi_2 + \gamma \pi_3 + \alpha \pi_4) \quad (5)$$

In 2017, Selvakumar and Dhinakaran made a modification on the proposed model by Chen et al. by introducing the term of interfacial layers surrounding the clusters [1]. This correlation is given as follows:

$$\mu_{nf}/\mu_{bf} = \left(1 - \left(\frac{\Phi_{ecl}}{\Phi_m}\right)\right)^{[\eta]\Phi_m} \quad (6)$$

$$\Phi_{ecl} = \Phi_{cl}(1 + \beta) \quad (7)$$

where  $\Phi_{ecl}$  is the effective volume fraction of the clusters with interfacial layers, and  $\beta$  is the ratio of the interfacial layer thickness to the average cluster radius.

### 3. Summary of experimental studies

Dependence of the viscosity of nanofluids on the nanoparticle loading is widely studied as mentioned in the previous section. The viscosity of nanofluids containing various types of nanoparticles like metals, oxides, and carbon nanotubes has been examined against nanoparticle concentration. Despite extensive experimental studies on the effect of nanoparticle loading on the viscosity of nanofluids, there is no universal equation that can predict this property with high accuracy [2]. Moreover, almost all investigations on the viscosity of nanofluids showed an increase in viscosity with increasing nanoparticle volume fraction [3]. This is noticed in all formerly mentioned nanofluids, except for carbon nanotube-based nanofluids that exhibit inverse relation between viscosity and particle loading. In addition, Nadooshan et al. [4] in their comprehensive study on the rheological behavior of nanofluids have concluded that most nanofluids display Newtonian behavior at low volume fractions and non-Newtonian behavior at high nanoparticle volume fractions. Furthermore, it has been proven that increasing volume fraction can lead to clustering of nanoparticles, and accordingly the viscosity of the fluid will rise. This increase in viscosity is due to the increase in surface-to-volume ratio during the aggregate formation. Duan et al. [5] investigated the effect of aggregation on the viscosity of Al<sub>2</sub>O<sub>3</sub>-water nanofluids and the results confirmed an increase in relative viscosity with the growth of cluster formation. Gaganpreet and Srivastava [6] also studied the effect of particle size, particle volume concentration, and concentration of particle aggregation on viscosity. The results revealed that nanofluid's volume fraction does not affect the viscosity directly, and increasing particle loading will result in aggregates. Therefore, viscosity increases as the size of aggregation increases [7].

In all studies on viscosity dependence of temperature in literature, an inverse relationship between viscosity and temperature has been observed, except for few works that show antithetical results such as Prasher et al. [8]. Investigations on the temperature effect on the viscosity of nanofluids have not reached a universal formula that describes viscosity behavior of such complex fluids as a function of

temperature. This might be due to the effect of other factors such as the type of base fluid, volume fraction, and particles' size on viscosity. Therefore, it was found that using the relative viscosity term ( $\mu_{nf}/\mu_{bf}$ ) is more beneficial over using the viscosity in its absolute scale, which results in an easier understanding about the dependence of viscosity on temperature [2].

In all early cited studies, the relative viscosity was almost stable with temperature increase at low to moderate particle loading for nearly all nanofluid types, while at high nanoparticle concentrations, the relative viscosity starts to increase with increasing temperature. Few studies showed hysteresis in relative viscosity of nanofluids with temperature, where the relative viscosity started to increase and then decrease with increasing temperature. This behavior can be seen in the study done by Namburu et al. [9] for 29-nm CuO-(60:40) EG/water nanofluid. Other researchers concluded a reduction in relative viscosity with increasing temperature like the study of Li et al. [10] on ZnO-EG nanofluids. Investigations on the size effect of nanoparticles on the viscosity of nanofluids are few, and this can be referred to three reasons. The first reason is that measurements should be conducted, at the same time, for at least three nanoparticle sizes of the same type of nanofluids in the same base fluid. Secondly, the investigator should monitor with great attention particle distribution within the base fluid, and finally, perhaps many investigators have been frustrated by contradictory results on viscosity dependence on nanoparticles' size. Most studies on the influence of the size of nanoparticles showed a decrease in viscosity with increasing particle size. However, other studies have shown conflicting information. He et al.'s [11] and Nguyen et al.'s [12] studies showed a direct relation of viscosity with nanoparticles' size. Moreover, Nguyen et al. [12] have stated that at relatively low particle loading, nanoparticles' sizes have no virtual effect on the viscosity of nanofluids. Moreover, as nanoparticles' content increases, the effect of particles' size becomes significant and the higher viscosity will correspond to nanofluids of larger nanoparticle size. Prasher et al. [8], on the other hand, showed no significant effect on the viscosity of nanofluids by the size of nanoparticles. These discrepancies can be due to the variations in the production and measurement methods of various studies in the literature. Additionally, particle size range at each study is limited, and usually, two to three particle sizes are studied at a time that makes it difficult to evaluate the dependence of viscosity on particles' size. Furthermore, the addition of surfactants or other additives to nanofluids may affect the interpretation on particles' size dependence of viscosity, especially at high temperature where the interaction between nanoparticles and surfactant molecules is affected. The shape of nanoparticles is also an issue. If the particle sizes or diameters are the same but the shapes are different, such as spherical and rod-like, then viscosity and other properties will differ [13].

## **4. Experimental work**

The viscosity of nanofluids is a function of many factors. Many researchers have considered a variety of such factors including type and size of the nanoparticle, compositional nature of the nanofluid mixture, as well as the temperature and pH of the mixture. The goal of this contribution is to examine and determine the effect of such variables on the dynamic viscosity of two types of nanofluids.

### **4.1 Selection of materials used**

The fluids were purchased from the US Research Nanomaterials Company. This study focuses on the effect of particle size besides the effect of the nanoparticle

concentration and temperature. Therefore, the nanofluids used in this analysis were selected based on their particle size and type. Graphene-DI water dispersion was selected as a nonmetallic nanoparticle dispersion, and three ferrous oxide (Fe<sub>2</sub>O<sub>3</sub>)-DI water dispersions of different nanoparticle sizes were chosen as metallic oxide nanofluids. Graphene-DI water nanofluid has a weight fraction of 1%, a thickness between 0.55 and 1.2 nm, a diameter between 1 and 12 μm, specific surface area in the range of 500–1200 m<sup>2</sup>/g, and a purity of 99.3%. The true density of the graphene was not provided by the supplier, and in this case, it was assumed to be 1 g/cm<sup>3</sup>, for the sake of simplicity, as it has been found in the literature. Graphene is in sheet form of two-dimensional structures. It has excellent mechanical, thermal, and electrical properties. However, it is difficult to disperse graphene due to its large surface area. The US Research Nanomaterials Company labs are using a high-capacity ultrasonic equipment to disperse graphene in the specific dispersant, and the results show a very uniform and stable nanofluid. Three different particle sizes of ferrous oxide (Fe<sub>2</sub>O<sub>3</sub>) dispersed in DI water have been selected: 5, 10, and 30 nm. All iron oxides were dispersed in deionized water using a laser synthesizing method. Both 5- and 10-nm (Fe<sub>2</sub>O<sub>3</sub>)-DI water nanofluids have a weight fraction of 15 wt%, while 30-nm (Fe<sub>2</sub>O<sub>3</sub>)-DI water nanofluid has a weight fraction of 20 wt%. The purity of 5- and 10-nm nanofluids is 99.9%, whereas the 30-nm dispersion has a purity of 99.5%. The molar mass of nanoparticles is 159.69 g/mol and they have a true density of 5.24 g/cm<sup>3</sup>. They are all spherical in shape. Five samples of graphene-DI water were prepared and they have volume fractions of 0.15, 0.45, 0.65, 0.85, and 1.00%. For iron oxide-DI water, the volume fractions were selected based on the stability of the diluted nanofluids and in a suitable range of volume fractions where other models of iron oxide nanofluid have been developed. The chosen volume concentrations for all three sets of Fe<sub>2</sub>O<sub>3</sub>-DI water were the same in order to examine the effect of particle size on viscosity. All prepared samples were ultrasonicated for around 2 hours at room temperature to ensure homogeneity and stability. Whenever these samples were kept for a long time, they were re-sonicated for 30 minutes to 1 hour prior to any measurement.

#### 4.2 Zeta potential measurements

The second step was to take the readings of zeta potentials for all samples to confirm the stability of nanofluid samples. Zeta potential apparatus identifies the net charge on the nanoparticles, and accordingly gives an idea about the superficial properties of those particles in a suspension. The concept behind the zeta potential is that the ionized particles in a suspension are surrounded by two counter ion layers of the dispersant. The first film-like layer is called the Stern layer, while, the other loosely attached ions make up the diffusive ion layer, where ions' arrangement in this layer is affected by the thermal movements and electrical forces. As nanoparticles move in the dispersing fluid, the ions in the diffusive ion layer keep moving with the particle that they are associated to, separated from those ions in the liquid phase as if there is a boundary between them. This boundary is called the slipping plane. The difference in potentials between the slipping plane around those particles and fluid medium is the electrokinetic potential or in other words zeta potential  $\zeta$ . When zeta potential value ( $\zeta$ ) between a point in the liquid phase and the slipping plane of particles is high (negative or positive), this will result in a high resistance of nanoparticles to agglomerate and vice versa. Therefore, zeta potential measurement is considered as an aid to identify the agglomeration of particles and, consequently, the stability of the nanofluid. Usually, when low zeta potential ( $\pm\zeta$ ) of less than 25 mV is reported, this means the colloidal suspensions in the fluid tend to flocculate and thus the nanofluid is unstable. Zeta potential values ( $\pm\zeta$ ) of

nanofluids between 30 and 40 mV are associated with a poorly stable suspension, while values ranging between 40 and 60 mV indicate good, stable suspensions, and those greater than 60 mV signify highly stable nanofluids. Hence, the zeta potential data have great advantages in commenting on the stability of the samples under study. Graphene-based nanofluids have an average zeta potential value ranging from 60 to 80, which is a signpost of excellent stability of the suspension. On the other hand, iron oxide samples showed fluctuating behavior. For instance, the average zeta potential value of 5 nm Fe<sub>2</sub>O<sub>3</sub> in DI water is fluctuating in the approximate range of 70 to 290 mV. Overall, this indicates a highly stable 5-nm Fe<sub>2</sub>O<sub>3</sub> nanofluid. The same thing is observed with the other two sets of Fe<sub>2</sub>O<sub>3</sub>-DI water. In the 10-nm Fe<sub>2</sub>O<sub>3</sub>-DI water system, the values of zeta potential are between 180 and 370 mV, while in the 30-nm Fe<sub>2</sub>O<sub>3</sub>-DI water system, there is a narrow range of potential between 270 and 350 mV. It is worth mentioning that the 30-nm Fe<sub>2</sub>O<sub>3</sub>-DI water nanofluid is highly stable, and the particles have no tendency to settle down even after a long time. However, in the 5-nm Fe<sub>2</sub>O<sub>3</sub>-DI water and 10-nm Fe<sub>2</sub>O<sub>3</sub>-DI water nanofluids, the nanoparticles lean toward settling down after a long time of around 1 hour after ultrasonication.

### 4.3 Viscosity measurements

The viscosity was measured by Cannon-Fenske capillary viscometer. The viscosity of the lowest and highest concentrations of graphene-based nanofluids was measured first to indicate the size of the capillary tube suitable for the rest of the measurements. The same step was repeated just with the Fe<sub>2</sub>O<sub>3</sub> (size 5 nm) system. The viscosities of other ferrous oxide-based nanofluids were measured using the same capillary tube size. However, the Fe<sub>2</sub>O<sub>3</sub> nanofluid of 30-nm particle size shows very low viscosity close to that of water. A thermostatic bath was used to regulate the surrounding temperature. The viscosity of all nanofluids was measured at temperatures of 25, 35, 45, 55, and 65°C. At each specific concentration and temperature, three readings of time which the fluid takes to flow from the upper mark to the lower mark of the capillary tube are taken. Viscosity measurement experiments have been conducted two times to check the results, and the averages of the two experiments have been calculated. The time is then converted to the kinematic viscosity by the following equation:

$$\nu = C \times t \quad (8)$$

where  $\nu$  is the kinematic viscosity in (cSt),  $C$  is an approximate constant specified for each capillary viscometer in (cSt/s), and  $t$  is the time in (s). The kinematic viscosity can be defined as the ratio between the dynamic or absolute viscosity ( $\mu$ ) in (cp) and bulk density ( $\rho_{bulk}$ ) in (g/cm<sup>3</sup>) as stated in Eq. (9). The true density of all samples was provided by the US Research Nanomaterials Company, and it was 1 (g/cm<sup>3</sup>) for all samples; therefore, kinematic viscosity and absolute viscosity are equal.

$$\nu = \frac{\mu}{\rho_{bulk}} \quad (9)$$

The results of the viscosity measurements are given in **Table 1**. The averages of the time of both experiments have been calculated, and the corresponding average viscosities at each volume fraction of nanoparticles and temperature are listed in **Table 1**. The standard deviation was also calculated for all viscosity readings of various samples at different temperatures using Eq. (10). For graphene-based

Nanofluid type (vol. %)	T (°C)	Experiment 1			Experiment 2			Average time (s)	Average viscosity (cp)
		Time readings (s)			Time readings (s)				
		1st	2nd	3rd	1st	2nd	3rd		
Graphene (0.15)	25	250.70	250.40	247.70	249.90	249.60	252.10	250.07	1.00
	35	201.80	204.73	205.08	207.80	205.93	205.78	205.18	0.82
	45	170.27	168.65	168.87	170.67	171.75	172.13	170.39	0.68
	55	143.77	143.28	142.30	146.37	148.73	147.70	145.36	0.58
	65	122.90	123.27	123.03	128.43	127.93	129.23	125.80	0.50
Graphene (0.45)	25	318.63	318.80	319.63	325.43	324.60	321.97	321.51	1.29
	35	260.00	258.41	258.90	260.93	260.85	261.23	260.06	1.04
	45	214.35	214.55	213.15	216.79	218.05	217.25	215.69	0.86
	55	181.30	182.73	182.53	183.49	183.93	182.93	182.82	0.73
	65	157.37	156.93	157.71	157.97	158.33	158.81	157.85	0.63
Graphene (0.65)	25	389.06	388.90	388.92	390.34	388.90	389.29	389.23	1.56
	35	313.48	314.35	315.70	313.73	314.71	316.16	314.68	1.26
	45	257.70	259.60	260.38	258.60	260.90	261.12	259.72	1.04
	55	217.63	217.77	218.39	219.67	218.49	219.11	218.51	0.87
	65	186.59	187.60	188.20	187.57	196.00	189.50	189.24	0.76
Graphene (0.85)	25	442.90	445.70	444.00	444.10	452.60	444.60	445.65	1.78
	35	357.95	357.38	358.08	359.25	357.13	356.28	357.68	1.43
	45	298.70	294.46	293.01	298.36	294.94	293.39	295.48	1.18
	55	249.57	245.32	250.05	249.58	245.48	248.85	248.14	0.99
	65	210.28	214.00	212.93	210.58	220.20	217.53	214.25	0.86
Graphene (1.00)	25	518.03	512.88	511.70	512.77	513.92	507.50	512.80	2.05
	35	415.14	414.23	414.85	415.56	416.73	410.95	414.58	1.66
	45	341.68	341.43	339.68	342.98	342.93	341.52	341.70	1.37
	55	287.22	289.43	287.92	286.98	288.67	286.58	287.80	1.15
	65	245.26	246.22	247.53	246.26	246.58	247.78	246.60	0.99
5-nm Fe <sub>2</sub> O <sub>3</sub> (0.19)	25	345.70	348.28	360.18	343.06	337.00	405.38	356.60	1.43
	35	284.68	299.64	283.23	291.88	317.24	272.25	291.49	1.17
	45	233.60	230.72	235.91	222.32	234.28	241.01	232.97	0.93
	55	195.90	187.19	194.77	199.06	187.97	207.57	195.41	0.78
	65	158.00	158.98	170.48	165.88	164.86	165.80	164.00	0.66
5-nm Fe <sub>2</sub> O <sub>3</sub> (0.29)	25	418.19	417.38	411.18	410.85	423.66	418.26	416.59	1.67
	35	328.32	350.46	383.52	339.52	334.86	337.92	345.77	1.38
	45	259.23	263.60	268.28	267.43	264.10	287.62	268.38	1.07
	55	222.13	218.10	223.89	228.17	224.23	231.01	224.59	0.90
	65	188.43	187.20	174.10	180.30	203.33	178.90	185.38	0.74
5-nm Fe <sub>2</sub> O <sub>3</sub> (0.38)	25	523.26	523.85	522.28	529.10	512.59	526.35	522.91	2.09
	35	406.90	403.15	406.09	407.57	407.28	409.11	406.68	1.63
	45	322.94	318.47	320.18	318.79	316.60	316.25	318.87	1.28



Nanofluid type (vol. %)	T (°C)	Experiment 1			Experiment 2			Average time (s)	Average viscosity (cp)
		Time readings (s)			Time readings (s)				
		1st	2nd	3rd	1st	2nd	3rd		
5-nm Fe <sub>2</sub> O <sub>3</sub> (0.48)	55	259.10	258.05	260.15	264.30	259.78	263.68	260.84	1.04
	65	217.54	217.55	216.57	213.46	210.19	213.77	214.84	0.86
	25	618.98	610.76	628.52	653.46	611.01	616.80	623.25	2.49
	35	467.39	474.10	476.73	476.51	477.00	479.23	475.16	1.90
	45	361.17	364.45	359.74	368.33	367.12	363.13	363.99	1.46
	55	282.21	294.03	282.59	285.49	282.61	277.41	284.06	1.14
5-nm Fe <sub>2</sub> O <sub>3</sub> (0.57)	65	232.76	232.05	235.66	235.45	240.95	239.01	235.98	0.94
	25	771.14	774.59	772.17	773.82	770.81	767.10	771.60	3.09
	35	582.45	579.27	579.10	579.35	583.06	583.37	581.10	2.32
	45	430.28	433.95	432.11	432.92	437.02	393.79	426.68	1.71
	55	323.19	328.32	342.19	327.17	323.21	325.26	328.22	1.31
	65	269.22	271.84	272.04	276.15	273.60	258.92	270.29	1.08
10-nm Fe <sub>2</sub> O <sub>3</sub> (0.19)	25	345.13	344.75	347.30	348.41	340.22	343.93	344.96	1.38
	35	281.63	281.65	276.83	308.73	274.35	274.20	282.90	1.13
	45	222.12	229.38	218.33	220.75	221.66	223.64	222.64	0.89
	55	190.41	191.77	192.49	189.12	192.06	193.14	191.50	0.77
	65	162.82	162.24	162.48	168.11	160.87	162.53	163.17	0.65
	25	409.43	406.30	408.83	410.54	408.27	407.91	408.54	1.63
10-nm Fe <sub>2</sub> O <sub>3</sub> (0.29)	35	320.74	323.84	322.78	323.86	323.39	321.09	322.62	1.29
	45	254.38	258.13	259.79	255.49	251.67	255.28	255.79	1.02
	55	215.02	212.51	215.74	215.32	215.60	216.19	215.06	0.86
	65	180.16	180.20	178.89	181.24	185.30	182.34	181.36	0.73
	25	496.91	492.59	503.65	500.00	499.88	500.08	498.85	2.00
	35	390.19	391.83	392.82	393.28	386.54	393.11	391.29	1.57
10-nm Fe <sub>2</sub> O <sub>3</sub> (0.38)	45	299.54	303.98	304.68	302.39	307.65	305.79	304.01	1.22
	55	244.85	244.55	249.01	252.55	241.54	249.36	246.98	0.99
	65	203.05	205.77	204.25	206.08	210.04	203.75	205.49	0.82
	25	575.27	615.91	604.10	598.38	621.24	597.00	601.98	2.41
	35	464.59	466.14	469.81	466.91	472.86	459.29	466.60	1.87
	45	353.15	359.48	354.52	358.46	360.12	356.03	356.96	1.43
10-nm Fe <sub>2</sub> O <sub>3</sub> (0.48)	55	289.79	285.09	286.16	287.48	280.81	279.59	284.82	1.14
	65	236.61	237.00	234.25	235.54	237.90	236.55	236.31	0.95
	25	714.30	739.84	741.41	736.81	738.13	736.70	734.53	2.94
	35	548.79	548.98	548.72	549.32	548.28	549.01	548.85	2.20
	45	417.09	417.19	415.47	420.88	414.61	416.73	416.99	1.67
	55	320.33	324.88	328.10	321.04	319.04	325.37	323.13	1.29
10-nm Fe <sub>2</sub> O <sub>3</sub> (0.57)	65	263.47	265.29	266.99	263.94	262.78	268.38	265.14	1.06
	25	233.03	232.60	233.46	232.50	232.30	232.47	232.73	0.93
	35	188.83	191.92	188.56	189.30	189.38	192.54	190.09	0.76

Nanofluid type (vol. %)	T (°C)	Experiment 1			Experiment 2			Average time (s)	Average viscosity (cp)
		Time readings (s)			Time readings (s)				
		1st	2nd	3rd	1st	2nd	3rd		
	45	158.42	160.94	157.05	158.71	156.22	159.62	158.49	0.63
	55	134.85	136.83	133.57	134.41	129.54	135.61	134.14	0.54
	65	114.80	118.47	116.95	117.53	117.50	115.71	116.83	0.47
30-nm Fe <sub>2</sub> O <sub>3</sub> (0.29)	25	239.86	240.99	237.05	237.14	235.48	238.95	238.24	0.95
	35	191.74	193.20	194.00	195.66	195.17	195.56	194.22	0.78
	45	159.97	161.56	163.00	161.27	162.08	160.21	161.34	0.65
	55	137.24	135.68	137.24	137.83	139.32	136.73	137.34	0.55
	65	116.79	118.32	119.46	121.47	120.62	117.61	119.04	0.48
30-nm Fe <sub>2</sub> O <sub>3</sub> (0.38)	25	245.77	247.34	244.72	248.23	247.53	245.35	246.49	0.99
	35	201.66	201.49	200.33	201.71	201.84	202.34	201.56	0.81
	45	164.51	165.07	166.13	165.14	167.18	166.17	165.70	0.66
	55	138.33	140.10	140.10	140.20	140.15	139.23	139.69	0.56
	65	120.95	121.65	121.04	121.15	123.68	121.61	121.68	0.49
30-nm Fe <sub>2</sub> O <sub>3</sub> (0.48)	25	250.77	249.20	248.87	251.23	253.13	250.76	250.66	1.00
	35	206.93	207.65	207.57	207.73	207.68	206.93	207.42	0.83
	45	169.64	172.08	172.22	171.70	169.83	172.13	171.26	0.69
	55	142.51	141.89	143.99	143.24	144.36	144.07	143.34	0.57
	65	124.18	121.90	125.60	124.48	125.25	125.73	124.53	0.50
30-nm Fe <sub>2</sub> O <sub>3</sub> (0.57)	25	258.38	259.87	258.61	259.09	260.06	258.49	259.08	1.04
	35	211.78	211.84	211.60	212.15	212.49	211.27	211.86	0.85
	45	175.71	174.29	174.04	176.14	175.46	175.86	175.25	0.70
	55	147.61	145.43	145.85	148.32	146.82	146.41	146.74	0.59
	65	128.39	127.24	126.91	129.12	126.87	128.04	127.76	0.51

**Table 1.**  
 Viscosity measurements for all nanofluid samples.

nanofluids, the average standard deviation was 1.88, while for iron oxide-based nanofluids, it was 4.22.

$$s = \sqrt{\frac{\sum_{i=1}^N (x_i - \bar{x})^2}{N - 1}} \quad (10)$$

As shown in **Figure 1**, five graphene-based nanofluids at different concentrations (0.15, 0.45, 0.65, 0.85, and 1.00%) were tested under five different temperatures, which are 25, 35, 45, 55, and 65°C. It can be observed that as the temperature increases, the viscosity declines. Moreover, the viscosity rises with the increasing concentration. Since the stepwise increase between concentrations is the same, it can be seen that the gradual increase in viscosity is almost equal between any concentration and the one above. **Figures 2–4** present viscosity measurements for the iron oxide-based nanofluids for the particle sizes of 5, 10, and 30 nm,

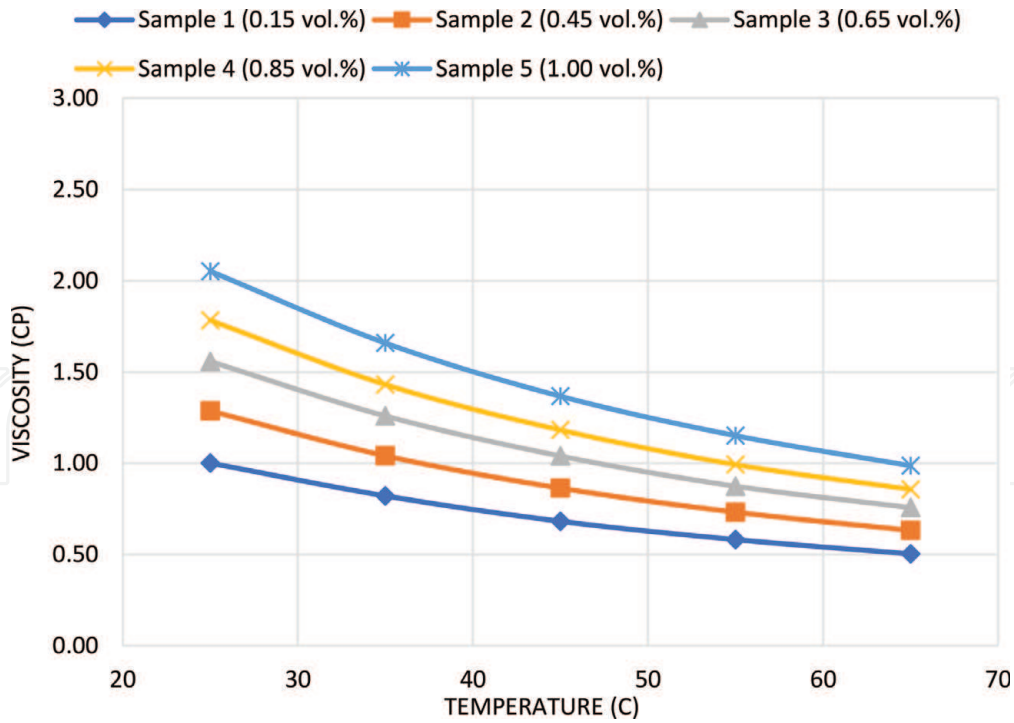


**Figure 1.**  
Viscosity measurements of graphene samples.

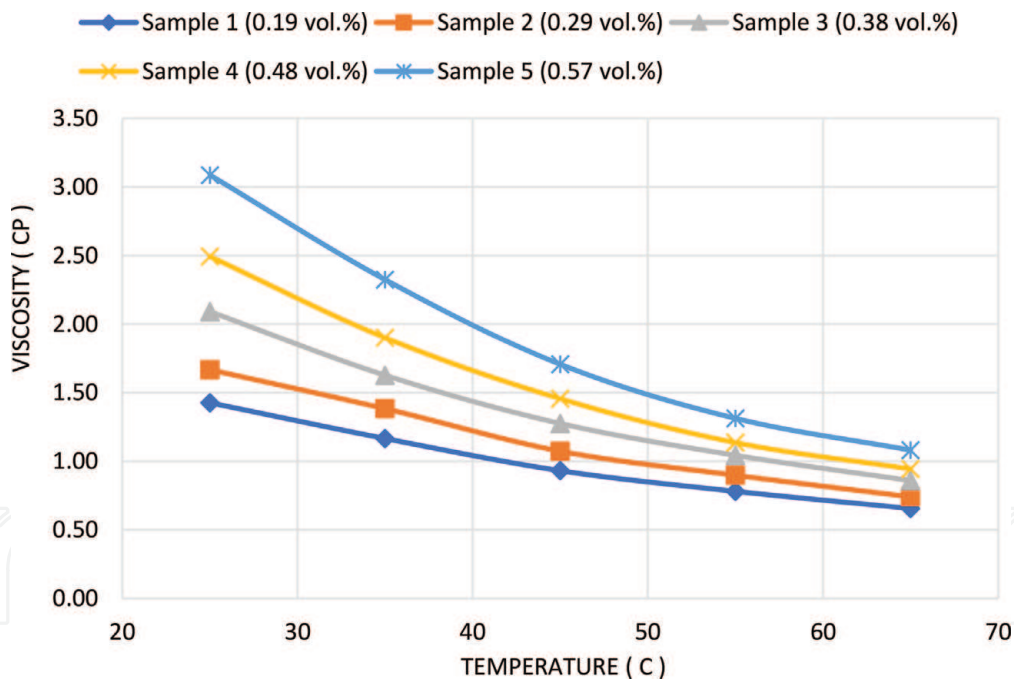


**Figure 2.**  
Viscosity measurements of 5-nm Fe<sub>2</sub>O<sub>3</sub>-based nanofluid.

respectively. It is observed that the viscosity increases with the increase of concentration and with the decrease in temperature. It is also noticed that there is a slight increase in the viscosities of 5-nm Fe<sub>2</sub>O<sub>3</sub> nanofluid compared with 10-nm Fe<sub>2</sub>O<sub>3</sub> nanofluid.

It is observed that the viscosity increases with the increase of concentration and with decrease in temperature. Furthermore, it is observed that there is a gradual increase in the difference between any two lines, knowing that the stepwise increase in the concentration is even, at the same temperature for a given nanofluid. In many studies on the effect of nanoparticle size on the viscosity of a fluid, it was found that at very low volume fractions, the effect of particle size is not significant,

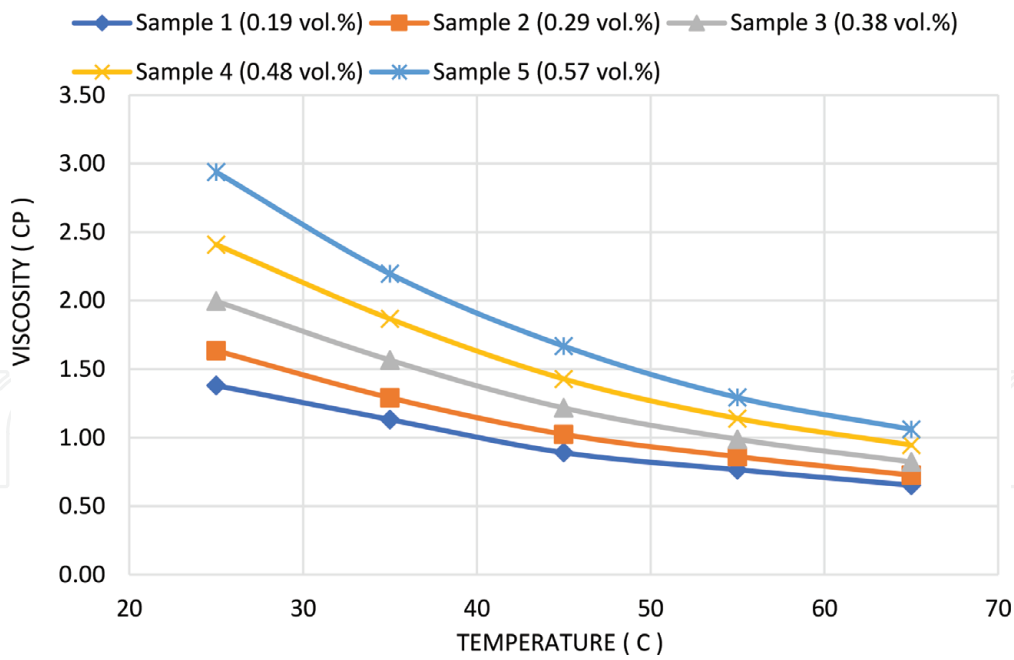


**Figure 3.**  
 Viscosity measurements of 10-nm  $Fe_2O_3$ -based nanofluid.

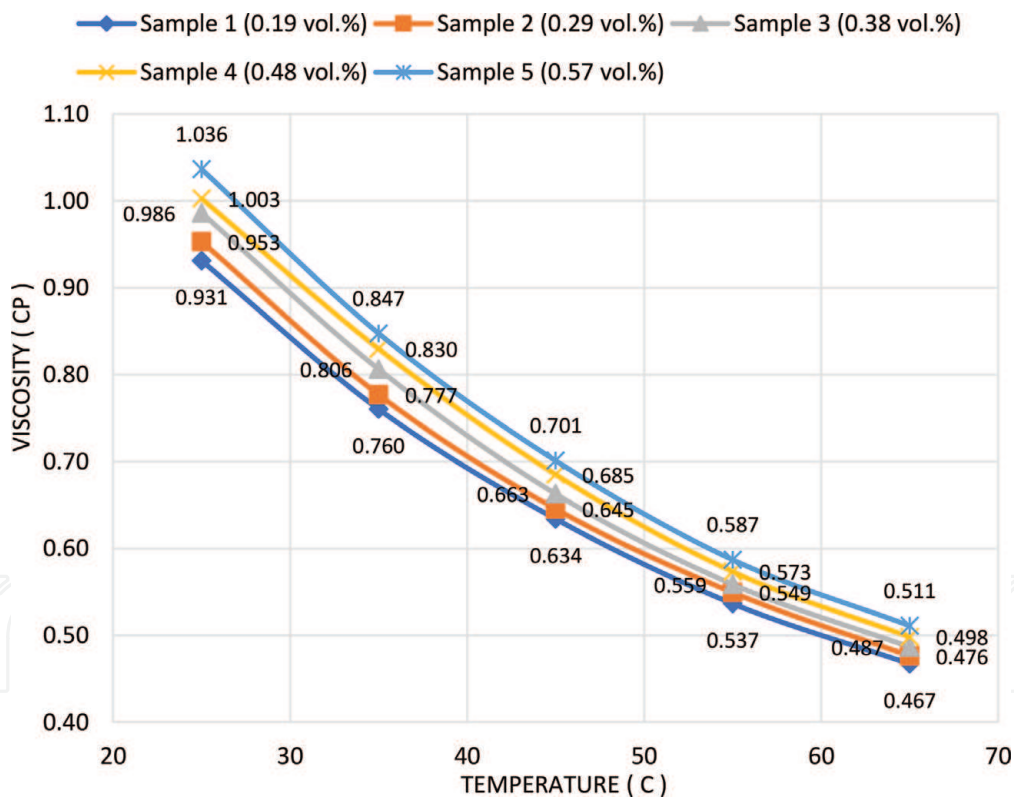


**Figure 4.**  
 Viscosity measurements of 30-nm  $Fe_2O_3$ -based nanofluid.

and at higher volume concentrations, the effect becomes more obvious. For example, when two aluminum oxide water nanofluids have a different particle size of 36 and 47 nm, and the same volume fraction of less than 4 vol%, the measured viscosities of both are virtually equal. But when the volume fraction has increased beyond 4 vol%, the viscosity of 36-nm  $Al_2O_3$ -water nanofluid is much higher than that of 47-nm  $Al_2O_3$ -water nanofluid. Few studies have been carried out to see the effect of particle size on the viscosity of nanofluids. Some of them concluded a reduction in viscosity with decreasing particle size like for the system of  $TiO_2$ -water

nanofluids with relatively large particle size (95, 132, and 230 nm) and low concentrations of less than 1.2 vol%. Many other studies have found an inverse relation between nanoparticle size and viscosity of nanofluid such as Namburu et al.'s study on aluminum oxide ethylene glycol-based nanofluid, Rudyak's experimental research on silicon oxide water-based nanofluids, and molecular dynamics simulations of Vakili-Nezhaad et al. [40, 41]. Until now, there has been no distinct explanation for this behavior of nanofluids.

## 5. Modeling and analysis

### 5.1 Calculating viscosity of nanofluids using models from literature

Since there are few models on the effect of nanoparticle size on viscosity along with the temperature and volume concentration factors, four models have been selected to reproduce the relative viscosity of graphene and ferrous oxide-based nanofluids. Three of them predict viscosity as a function of temperature, volume fraction, and size of nanoparticles. These models have been selected based on their specifications of nanoparticle material, base fluid, temperature range, and volume fraction. All chosen equations consider nonmetallic or metal oxide nanoparticles, which are dispersed in water at low volume fractions of less than 9 vol%, and viscosity is measured at temperatures ranging between 20 and 90°C. Average absolute deviations were calculated by Eq. (11) to comment on and verify the accuracy of the models.

$$AAD\% = \frac{1}{n} \left\{ \sum_{i=1}^n \left| \frac{(\mu_r)_{exp} - (\mu_r)_{prd}}{(\mu_r)_{exp}} \times 100 \right| \right\} \quad (11)$$

The first model is that of Azmi et al. [14]. They have proposed Eq. (12) for the viscosity of Al<sub>2</sub>O<sub>3</sub> and CuO nanoparticle in water as base fluid. Here,  $\mu_{nf}$  and  $\mu_w$  are the viscosity of nanofluid and water in cp,  $T_{nf}$  and  $T_w$  are temperatures of nanofluid and water in °C,  $\Phi_p$  is the volume fraction of nanoparticles, and  $d_p$  is nanoparticles' size in nm.

$$\mu_{nf} = \mu_w \left( 1 + \frac{\Phi}{100} \right)^{11.3} \left( 1 + \frac{T_{nf}}{70} \right)^{-0.038} \left( 1 + \frac{d_p}{170} \right)^{-0.061} \quad (12)$$

$$\mu_w = 0.00169 - 4.25263e - 5 \times T_w + 4.9255e - 7 \times (T_w)^2 - 2.09935e - 9 \times (T_w)^3 \quad (13)$$

In this model, experimental results are taken from the works of Wang et al. [15], Pak and Cho [16], Zeinali Heris et al. [17], Nguyen et al. [12], He et al., (2007), Nguyen et al. [18], Lee et al. [19], Hwang et al. [20], Duangthongsuk and Wongwises [21], and Lee et al. [22] to build a new nonlinear regression equation. In these experimental works, the particles' sizes of aluminum oxide are 36 and 47 nm, while the particle size of copper oxide is 29 nm. All volume fractions that have been investigated are less than 4%, and viscosity was measured at ambient temperature. Eq. (12) has shown an average absolute deviation of 2.89% for calculating the viscosity of Al<sub>2</sub>O<sub>3</sub> and CuO nanoparticles in water as base fluid. However, when it was used to calculate the viscosity of all ferrous oxide nanoparticles, the average absolute deviation (AAD%) was 38.48%. Moreover, it was observed that the lowest AAD% was that calculated for 30-nm Fe<sub>2</sub>O<sub>3</sub>-based nanofluids in water, where the particle size of this nanofluid is close to that of Al<sub>2</sub>O<sub>3</sub>-water and CuO-water

nanofluids used to generate this model. For graphene, the average absolute deviation (AAD%) between the experimental data and estimated viscosity using Eq. (12) was 41.02%. The second model is proposed by Khanafer and Vafai [23], and given by Eq. (14), where  $\mu_{eff}$  is the dynamic viscosity of nanofluid in mPa.s (1 cp = 1 mPa.s),  $T$  is the temperature in °C,  $\Phi_p$  is the volume fraction of nanoparticles, and  $d_p$  is nanoparticles' size in nm.

$$\mu_{eff} = -0.4491 + \frac{28.837}{T} + 0.574\Phi_p - 0.1634\Phi_p^2 + 23.053\frac{\Phi_p^2}{T^2} + 0.0132\Phi_p^3 - 2354.735\frac{\Phi_p}{T^3} + 23.498\frac{\Phi_p}{d_p^2} - 3.0185\frac{\Phi_p^3}{d_p^2} \quad (14)$$

This equation estimates the viscosity of various Al<sub>2</sub>O<sub>3</sub>-water nanofluids with volume fractions between 1 and 9% with particle size ranges from 13 to 131 nm, and at temperatures between 20 and 70°C. This equation was developed using various viscosity data of Al<sub>2</sub>O<sub>3</sub>-water in the literature which are presented in Koblinski et al. [24], Putra et al. [25], Nguyen et al. [12], and Anoop et al. [26]. Khanafer and Vafai [23] have stated that their regression equation shows a correlation coefficient of ( $R^2$ ) of 99% for all experimental data of Al<sub>2</sub>O<sub>3</sub>-water nanofluids. When Khanafer and Vafai's [23] model was used to find the viscosity of all Fe<sub>2</sub>O<sub>3</sub>-deionized water nanofluids of our work at different conditions of temperatures and volume fractions, a 78.10% average absolute deviation (AAD%) was observed. For our graphene-based nanofluids, the AAD% was 77.74%. In both cases, the error was too high.

The model proposed by Sekhar and Sharma [27] is the third model used to predict the viscosity of the nanofluids of this study, and their correlation is shown in Eq. (15) below, where  $\mu_r$  is the relative viscosity of the nanofluid to its base fluid,  $\Phi$  is the volume fraction of nanoparticles,  $T_{nf}$  is the temperature in °C, and  $d_p$  is nanoparticles' size in nm.

$$\mu_r = 0.935 \left(1 + \frac{T_{nf}}{70}\right)^{0.5602} \left(1 + \frac{d_p}{80}\right)^{-0.05915} \left(1 + \frac{\Phi}{100}\right)^{10.51} \quad (15)$$

Sekhar and Sharma referred to experimental measurements of Al<sub>2</sub>O<sub>3</sub>-water nanofluids' viscosity in literature, to cover diverse particle sizes, volume fractions, and temperatures. They have considered experimental data for viscosity of Al<sub>2</sub>O<sub>3</sub>-water nanofluids from studies of Pak and Cho [16], Das et al. [28], Prasher et al. [8], Jang et al. [29], Timofeeva et al. [30], Lee et al. [19], Williams et al. [31], Nguyen et al. [18], Tavman et al. [32], Anoop et al. [26], Chandrasekar et al. [33], Duan et al. [5], and Murshed [34] along with their measurements to develop Eq. (15). Therefore, this equation can predict the viscosity of Al<sub>2</sub>O<sub>3</sub>-water nanofluids of 13–100 nm particle size and volume fraction ranges between 0.01 and 5%, at temperature ranges from 20 to 70°C. This model has an average absolute deviation of 9% with all Al<sub>2</sub>O<sub>3</sub>-water nanofluids' experimental data of viscosity. Regarding our experimental data, a large deviation (AAD%) of 29.32 and 23.43% was shown when the viscosity of Fe<sub>2</sub>O<sub>3</sub>-deionized water and graphene-deionized water nanofluids was calculated using Eq. (15), respectively. The deviation between the calculated viscosity and the experimental results was the lowest for 30-nm Fe<sub>2</sub>O<sub>3</sub>-deionized water nanofluids (average 12.93%), while in other nanofluids the error was much higher.

The fourth examined model is the model developed by Ahammed et al. [35] for graphene-water-based nanofluids of 1–5-nm particle thickness. This model is presented in Eq. (16). It is obvious that this equation of relative viscosity is a

Model	5-nm Fe <sub>2</sub> O <sub>3</sub> -DI water	10-nm Fe <sub>2</sub> O <sub>3</sub> -DI water	30-nm Fe <sub>2</sub> O <sub>3</sub> -DI water	All Fe <sub>2</sub> O <sub>3</sub> -DI water nanofluids	0.875-nm graphene-DI water
Azmi et al. [14]	52.12	51.15	11.51	38.48	41.02
Khanafer and Vafai [23]	82.24	82.95	67.76	78.10	77.74
Sekhar and Sharma [27]	37.97	36.64	12.93	29.32	23.43
Ahammed et al. [35]	18.43	16.67	52.73	29.50	13.91

**Table 2.**

*Average absolute deviations (%) between measured relative viscosities and estimated relative viscosities using different models for all Fe<sub>2</sub>O<sub>3</sub>- and graphene-based nanofluids in the present study.*

function of two variables: temperature and volume fraction.  $T_{\infty}$  and  $T$  are the ambient temperature and nanofluid temperature in °C, respectively, and  $\Phi$  is the volume fraction.

$$\frac{\mu_{nf}}{\mu_{bf}} = 4.682 \left( \frac{T_{\infty}}{T} \right)^{0.00049} \Phi^{0.1794} \quad (16)$$

In this model, measurement of the viscosity was for three different volume fractions of graphene: 0.05, 0.1, and 0.15%, at nine temperatures between 10 and 90°C. The measured viscosities have an average absolute deviation of 2% with the calculated viscosities by Eq. (16). Eq. (16) has been used in this research to predict the viscosities of all graphene and ferrous oxide-based nanofluids. The correlation predicts the viscosity of the graphene-based nanofluids and all Fe<sub>2</sub>O<sub>3</sub>-deionized water nanofluids with the AAD% of 13.91 and 29.5%, respectively. It is also noticed that Eq. (16) represents the viscosity of 5- and 10-nm Fe<sub>2</sub>O<sub>3</sub>-deionized water nanofluids better than its prediction for the viscosity of 30-nm Fe<sub>2</sub>O<sub>3</sub>-deionized water nanofluids. Furthermore, it was expected that this equation will give better predictions of graphene-DI water nanofluid of our study; however, the deviation somehow was high (13.91%). **Table 2** shows the average absolute deviation (AAD%) between the predicted viscosities by all four models and our experimental data of all graphene and ferrous oxide water-based nanofluids.

## 5.2 Development of a new model for the viscosity of nanofluids

In this section, we aim to develop a new correlation for calculation of the viscosity of our nanofluids with higher accuracy compared to the models available in the literature. The model was developed based on Vaschy-Buckingham theorem or dimensionless analysis theorem, which will be elaborated here in brief. In Vaschy-Buckingham theorem or dimensionless analysis theorem, any equation that describes a physical phenomenon includes a number of (n) variables that can be rewritten as (n-k) independent dimensionless coefficients ( $\pi$ ), where (n) is all physical quantities that are related or have effect on any physical phenomenon and k corresponds to the number of base quantities or fundamental dimensions such as dimensions of mass, length, and time for the mechanical system. In 1914, Buckingham [36] stated that any physical equation of different kinds of physical quantities can be written in the following form,

$$f(Q_1, Q_2, Q_3, \dots, Q_n) = 0 \quad (17)$$

If the physical equation contains some several quantities of any kind, the equation will be in form (18), in which  $r', r'' \dots$  etc. are the ratios of each one of these quantities to a chosen quantity of the same kind.

$$f(Q_1, Q_2, Q_3, \dots, Q_n, r', r'' \dots) = 0 \quad (18)$$

At this stage, let us focus on the form (18), assuming that there are no several quantities of the same kind. Every complete physical equation has the form (19).

$$\sum M Q_1^{b_1} Q_2^{b_2} \dots Q_n^{b_n} = 0 \quad (19)$$

According to the dimensional homogeneity's principle of Fourier, any physical equation must be homogenous in dimensions, which means each term in the equation must have the same dimension. This can be done through dividing Eq. (19) by any term; thus, the resulting equation will be in the form (20), where  $N$ s are dimensionless numbers, and  $a_1, a_2 \dots a_n$  are exponents that make all terms dimensionless (i.e.,  $a_1 + a_2 + \dots + a_n = 0$ )

$$\sum N Q_1^{a_1} Q_2^{a_2} \dots Q_n^{a_n} + 1 = 0 \quad (20)$$

Now, if

$$\pi = Q_1^{a_1} Q_2^{a_2} \dots Q_n^{a_n} \quad (21)$$

then, Eq. (20) will be in the form of Eq. (22)

$$\sum N \pi + 1 = 0 \quad (22)$$

Since  $\pi$  is dimensionless, the product of all  $\pi$ 's, let say,  $\pi_1^{x_1} \pi_2^{x_2} \dots \pi_i^{x_i}$ , will also be dimensionless. In other words, each  $\pi$  is, now, an independent dimensionless product of quantities  $Q$  in Eq. (21); hence, Eq. (22) can be rewritten in the form (23) and (24). Note that up to this stage Fourier principle is still satisfied. Moreover, according to Eq. (20) and (21), every  $\pi$  term equals 1 (i.e.,  $[\pi_1] = [\pi_2] = [\pi_3] = \dots = [\pi_i] = [1]$ , and  $\sum_{j=1}^n (x_j) = 0$ ).

$$\sum N \pi_1^{x_1} \pi_2^{x_2} \dots \pi_i^{x_i} + 1 = 0 \quad (23)$$

$$\psi(\pi_1, \pi_2, \pi_3, \dots, \pi_i) = 0 \quad (24)$$

The aim of the previous steps is to convert Eqs. (17)–(24) by combining different  $Q$  variables in various ways into dimensionless terms. After that, Buckingham gave a restriction for the maximum number of dimensionless terms (i). Buckingham assumed that  $k$  is the number of the fundamental dimensions,  $n$  is the number of quantities ( $Q$ s) that can be derived from the base quantities, and, thus,  $i$  equals  $(n-k)$ .

$$\left\{ \begin{array}{l} [\pi_1] = [Q_1^{\alpha_1} Q_2^{\beta_1} \dots Q_k^{\gamma_1} P_1] = [1] \\ [\pi_2] = [Q_1^{\alpha_2} Q_2^{\beta_2} \dots Q_k^{\gamma_2} P_2] = [1] \\ \dots\dots\dots \\ [\pi_i] = [Q_1^{\alpha_i} Q_2^{\beta_i} \dots Q_k^{\gamma_i} P_i] = [1] \end{array} \right\} \quad (25)$$



Eq. (25) shows the form of independent dimensionless terms of a physical phenomenon. In order to get each dimensionless term, take  $k$  number of different kind quantities and let them be  $Q_1$  to  $Q_k$  in all  $\pi$  equations. Then each remaining  $(n-k)$  of different kind quantities to be the  $(P's)$  terms in each  $\pi$  equation.  $Q's$  are chosen such that they contain all base dimensions like mass, length, and time. Furthermore, it should be noted that those dimensions are not built on the size of the base quantities (fundamental dimensions). They are just dependent on the interrelation between them. Additionally, choosing different combinations of different kind quantities to be  $Q_1$  to  $Q_k$  will result in a different structure of Eq. (24). In this study, it was assumed that the viscosity of a nanofluid is affected by the viscosity of the base fluid, particles' concentration, nanoparticles' diameter, particles' diameter of the base fluid, kinetic or thermal energy due to temperature ( $T$ ), and interaction between particles through zeta potential ( $\zeta$ ), and electron charge ( $e$ ) as stated in Eq. (26). Boltzmann's constant is considered to be the average kinetic energy of a particle due to the increase in temperature by 1 K. Although, both electron charge ( $e$ ) and Boltzmann's constant ( $k$ ) are constants, they are not dimensionless; thus, according to the Buckingham theorem, they are physical quantities that can be measured and derived from other quantities. Therefore, they appear in the following equation as two quantities.

$$f(\mu_{nf}, \mu_{bf}, \Phi, d_p, d_o, T, k, e, \zeta) = 0 \quad (26)$$

$\mu_{nf}$  and  $\mu_{bf}$  are the viscosities of the nanofluids and water in cp,  $T$  is nanofluids' temperature in K;  $\Phi$  is the volume fraction;  $d_p$  is nanoparticles' size in nm;  $d_o$  is the diameter of water molecule which is 0.275 nm;  $e$  is the electron charge which is  $1.60218 \times 10^{-19}$  C;  $\zeta$  is the zeta potential in V; and  $k$  is the Boltzmann constant,  $1.38066 \times 10^{-23}$  J/K. In this model, prediction of viscosity was enhanced by including a term, which consists of two factors,  $kT$  and  $e\zeta$ . A closer look at Eq. (26) reveals that we have seven different kinds of quantities. Since  $\mu_{nf}$  and  $\mu_{bf}$  are of the same kind, and  $d_p$  and  $d_o$  are also of the same kind; then, Eq. (26) will be in the form of Eq. (27). Consequently, the physical equation has  $(n)$  different kinds of quantities ( $n = 7$ ), where three of them are dimensionless ratios (i.e.,  $r' = \Phi$ ,  $r'' = \frac{\mu_{nf}}{\mu_{bf}}$ ,  $r''' = \frac{d_p}{d_o}$ ). The number of fundamental dimensions ( $k$ ) is 5; these are mass (M), time (T), length (L), temperature ( $\Theta$ ), and electrical current (I).

$$f(Q_1, Q_2, Q_3, Q_4, r', r'', r''') = f\left(T, k, e, \zeta, \Phi, \frac{\mu_{nf}}{\mu_{bf}}, \frac{d_p}{d_o}\right) = 0 \quad (27)$$

Eventually, based on the mentioned theory, the following form of function  $\varphi$  in Eq. (28) was obtained, in which all constants  $C_0$ ,  $C_1$ ,  $C_2$ , and  $C_3$  are empirical constants to be obtained by nonlinear regression analysis using experimental data set.

$$\frac{\mu_{nf}}{\mu_{bf}} = C_0 \Phi^{C_1} \left(\frac{d_p}{d_o}\right)^{C_2} \exp\left(\frac{C_3 e \zeta}{kT}\right) \quad (28)$$

Microsoft Excel was used to list all independent and dependent variables and all data of trials to get the best fit's coefficients, while MATLAB was used to import the data from Excel and find the best regression coefficient in each trial. Changing initial values, repeating trials, and calculating the average absolute deviation

between the expected and the predicted relative viscosity were repetitive processes used to get the best nonlinear regression model for the viscosity of nanofluids. The optimized parameters of  $C_0$ ,  $C_1$ ,  $C_2$ , and  $C_3$  which provide the best fit are tabulated in **Table 3** for both graphene- and  $Fe_2O_3$ -based nanofluids.

An average absolute deviation of 13.74% between the calculated relative viscosities by the new model and the experimental data for all iron oxide-based nanofluids was obtained. For graphene-based nanofluids, it was 5.82%. It is obvious that this model reduces the deviation for all types of nanofluids since it includes the nanoparticle's size effect besides the effect of kinetic and potential energies between nanoparticles. **Table 4** shows the overall average absolute deviations (AAD%) for all models from the literature and the new developed model in this research. It shows enhancement in estimating the viscosity of nanofluids by the new model.

A comparison between experimental data and calculated values by different models for graphene-based nanofluids was made. It was observed that most of the points calculated by the new model were in the range of  $-5$  to  $+5\%$  deviation from the experimental data resulting in an average absolute deviation of 5.82%. For the model proposed by Ahammed et al. [35], the calculated points are spread over a range of deviation from  $-10\%$  and higher than  $+20\%$ , resulting in an average absolute deviation of 13.91%. For the models of Sekhar and Sharma [27], Azmi et al. [14], and Khanafer and Vafai [23], most of the calculated points have deviations' ranges lower than  $-20\%$ . The average absolute deviations of those models are 23.43, 41.02, and 77.74% respectively, and they underestimate the viscosity of graphene-based nanofluids. A similar comparison was made between the experimental data and calculated values by different models for  $Fe_2O_3$ -based nanofluids. It was noticed that most of the points of the new model are widely spread over the range of  $-20$  to  $+20\%$  deviations which finally gives an average absolute deviation of 13.74%. The model proposed by Ahammed et al. [35]

Constant	All $Fe_2O_3$ -DI water nanofluids	Graphene-DI water nanofluids
$C_0$	191.791451	3.384594
$C_1$	0.590026	0.342364
$C_2$	$-0.414975$	0.674537
$C_3$	0.0165741	0.117727

**Table 3.**  
*Values of constants for the proposed new model.*

Model	All $Fe_2O_3$ -DI water nanofluids	Graphene-DI water nanofluids
Semi-empirical model (present work)	13.74%	5.82%
Ahammed et al. [35]	29.50%	13.91%
Sekhar and Sharma [27]	29.32%	23.43%
Azmi et al. [14]	38.48%	41.02%
Khanafer and Vafai [23]	78.10%	77.74%

**Table 4.**  
*Average absolute deviations between measured relative viscosities and predicted relative viscosities using different models for all  $Fe_2O_3$ - and graphene-based nanofluids.*

underestimates the relative viscosity of 5- and 10-nm-sized Fe<sub>2</sub>O<sub>3</sub>-based nanofluids, while it overestimates the relative viscosity of 30-nm Fe<sub>2</sub>O<sub>3</sub>-based nanofluids. Most data points for this model are in the range from 1% to over 30% deviations, which resulted in an average absolute deviation of 29.50%. For models of Sekhar and Sharma [27], Azmi et al. [14], and Khanafer and Vafai [23], most of the points were found to lie on the ranges lower than –20% deviations, which resulted in the average absolute deviations of 29.32, 38.48, and 78.10%, respectively. The models proposed by Azmi et al. [14] and Khanafer and Vafai [23] underestimate the relative viscosities of all Fe<sub>2</sub>O<sub>3</sub>-based nanofluids, while the model of Sekhar and Sharma [27] overestimates the relative viscosity of 30-nm Fe<sub>2</sub>O<sub>3</sub>-based nanofluids. The model proposed by Sekhar and Sharma [27] underestimates the relative viscosity of 5- and 10-nm Fe<sub>2</sub>O<sub>3</sub>-based nanofluids.

## **6. Conclusions**

This study focused on measuring the viscosity and analyzing the behavior of two types of nanofluids: ferrous oxide-DI water nanofluids (three sizes) and graphene-DI water nanofluids. The viscosity of graphene-based nanofluids was measured at different volume fractions of 0.15, 0.45, 0.65, 0.85, and 1.00%. We measured the viscosities of three different sizes of ferrous oxide-based nanofluids at volume fractions of 0.19, 0.29, 0.38, 0.48, and 0.57%. Zeta potential measurement was performed to check the stability of nanofluids, and all zeta potential values were above 60 mV, which indicates stable suspensions. All viscosity measurements were conducted using capillary viscometer at temperatures ranging between 25 and 65°C. Both types of nanofluids showed increasing viscosity with increasing nanoparticle loading, and decreasing viscosity with increasing temperatures. Furthermore, testing ferrous oxide-based nanofluids of different sizes revealed an inverse relation between the size of nanoparticles and viscosity. A total of 100 data points were generated and compared with the calculated values using the most relevant models available in the literature. All those models showed relatively high deviations from measured viscosities. Therefore, similar to other researches in this field, we developed a new model for the best fit with our experimental data. This model was developed using the Buckingham Pi theorem and it has a better performance compared to the other published models. It seems that there is still a long way to go to come up with a unified and universal model for the prediction of the viscosity of nanofluids because of the very complex nature of such materials.

IntechOpen

IntechOpen

### **Author details**

Majid Al-Wadhahi, G. Reza Vakili-Nezhaad\* and Ohoud Al Ghafri  
Petroleum and Chemical Engineering Department, College of Engineering,  
Sultan Qaboos University, Muscat, Oman

\*Address all correspondence to: [vakili@squ.edu.om](mailto:vakili@squ.edu.om)

### **IntechOpen**

---

© 2019 The Author(s). Licensee IntechOpen. This chapter is distributed under the terms of the Creative Commons Attribution License (<http://creativecommons.org/licenses/by/3.0>), which permits unrestricted use, distribution, and reproduction in any medium, provided the original work is properly cited. 

## References

- [1] Selvakumar RD, Dhinakaran S. Effective viscosity of nanofluids—A modified Krieger–Dougherty model based on particle size distribution (PSD) analysis. *Journal of Molecular Liquids*. 2017;**225**:20-27
- [2] Rudyak VY. Viscosity of nanofluids. Why it is not described by the classical theories. *Advances in Nanoparticles*. 2013;**2**(03):266
- [3] Mahbubul IM, Saidur R, Amalina MA. Latest developments on the viscosity of nanofluids. *International Journal of Heat and Mass Transfer*. 2012;**55**(4):874-885
- [4] Nadooshan AA, Eshgarf H, Afrand M. Evaluating the effects of different parameters on rheological behavior of nanofluids: A comprehensive review. *Powder Technology*. 2018;**338**: 342-353
- [5] Duan F, Kwek D, Crivoi A. Viscosity affected by nanoparticle aggregation in Al<sub>2</sub>O<sub>3</sub>-water nanofluids. *Nanoscale Research Letters*. 2011;**6**(1):248
- [6] Gaganpreet, Srivastava S. Effect of aggregation on thermal conductivity and viscosity of nanofluids. *Applied Nanoscience*. 2012;**2**:325-331
- [7] Ramachandran K, Kadirgama K, Awad OI, Ramasamy D, Samykano M, Azmi WH. Comprehensive review of principle factors for thermal conductivity and dynamic viscosity enhancement in thermal transport applications: An analytical tool approach. *International Communications in Heat and Mass Transfer*. 2018;**98**:13-21
- [8] Prasher R, Song D, Wang J, Phelan P. Measurements of nanofluid viscosity and its implications for thermal applications. *Applied Physics Letters*. 2006;**89**(13):133108
- [9] Namburu PK, Kulkarni DP, Misra D, Das DK. Viscosity of copper oxide nanoparticles dispersed in ethylene glycol and water mixture. *Experimental Thermal and Fluid Science*. 2007;**32**(2): 397-402
- [10] Li H, Wang L, He Y, Hu Y, Zhu J, Jiang B. Experimental investigation of thermal conductivity and viscosity of ethylene glycol based ZnO nanofluids. *Applied Thermal Engineering*. 2015;**88**: 363-368
- [11] He Y, Jin Y, Chen H, Ding Y, Cang D, Lu H. Heat transfer and flow behaviour of aqueous suspensions of TiO<sub>2</sub> nanoparticles (nanofluids) flowing upward through a vertical pipe. *International Journal of Heat and Mass Transfer*. 2007;**50**(11–12): 2272-2281
- [12] Nguyen CT, Desgranges F, Roy G, Galanis N, Maré T, Boucher S, et al. Temperature and particle-size dependent viscosity data for water-based nanofluids—hysteresis phenomenon. *International Journal of Heat and Fluid Flow*. 2007;**28**(6): 1492-1506
- [13] Koca HD, Doganay S, Turgut A, Tavman IH, Saidur R, Mahbubul IM. Effect of particle size on the viscosity of nanofluids: A review. *Renewable and Sustainable Energy Reviews*. 2017;**82**: 1664-1674
- [14] Azmi WH, Sharma KV, Mamat R, Alias ABS, Misnon II. Correlations for thermal conductivity and viscosity of water based nanofluids. In: *IOP Conference Series: Materials Science and Engineering* (Vol. 36, No. 1, p. 012029). IOP Publishing; 2012
- [15] Wang X, Xu X, Choi S, U S. Thermal conductivity of nanoparticle-fluid mixture. *Journal of Thermophysics and Heat Transfer*. 1999;**13**(4):474-480

- [16] Pak BC, Cho YI. Hydrodynamic and heat transfer study of dispersed fluids with submicron metallic oxide particles. *Experimental Heat Transfer*. 1998;**11**(2): 151-170
- [17] Zeinali Heris S, Razbani MA, Estellé P, Mahian O. Rheological behavior of zinc-oxide nanolubricants. *Journal of Dispersion Science and Technology*. 2015;**36**(8):1073-1079
- [18] Nguyen CT, Desgranges F, Galanis N, Roy G, Maré T, Boucher S, et al. Viscosity data for Al<sub>2</sub>O<sub>3</sub>-water nanofluid—Hysteresis: Is heat transfer enhancement using nanofluids reliable? *International Journal of Thermal Sciences*. 2008; **47**(2):103-111
- [19] Lee JH, Hwang KS, Jang SP, Lee BH, Kim JH, Choi SU, et al. Effective viscosities and thermal conductivities of aqueous nanofluids containing low volume concentrations of Al<sub>2</sub>O<sub>3</sub> nanoparticles. *International Journal of Heat and Mass Transfer*. 2008;**51** (11-12):2651-2656
- [20] Hwang KS, Jang SP, Choi SU. Flow and convective heat transfer characteristics of water-based Al<sub>2</sub>O<sub>3</sub> nanofluids in fully developed laminar flow regime. *International Journal of Heat and Mass Transfer*. 2009;**52**(1-2): 193-199
- [21] Duangthongsuk W, Wongwises S. An experimental study on the heat transfer performance and pressure drop of TiO<sub>2</sub>-water nanofluids flowing under a turbulent flow regime. *International Journal of Heat and Mass Transfer*. 2010;**53**(1-3): 334-344
- [22] Lee SW, Park SD, Kang S, Bang IC, Kim JH. Investigation of viscosity and thermal conductivity of SiC nanofluids for heat transfer applications. *International Journal of Heat and Mass Transfer*. 2011;**54**(1-3):433-438
- [23] Khanafer K, Vafai K. A critical synthesis of thermophysical characteristics of nanofluids. *International Journal of Heat and Mass Transfer*. 2011;**54**(19-20):4410-4428
- [24] Keblinski P, Phillpot SR, Choi SUS, Eastman JA. Mechanisms of heat flow in suspensions of nano-sized particles (nanofluids). *International Journal of Heat and Mass Transfer*. 2002;**45**(4): 855-863
- [25] Putra N, Roetzel W, Das SK. Natural convection of nano-fluids. *Heat and Mass Transfer*. 2003;**39**(8-9):775-784
- [26] Anoop KB, Kabelac S, Sundararajan T, Das SK. Rheological and flow characteristics of nanofluids: Influence of electroviscous effects and particle agglomeration. *Journal of Applied Physics*. 2009;**106**(3):034909
- [27] Sekhar YR, Sharma KV. Study of viscosity and specific heat capacity characteristics of water-based Al<sub>2</sub>O<sub>3</sub> nanofluids at low particle concentrations. *Journal of Experimental Nanoscience*. 2015;**10**(2):86-102
- [28] Das SK, Putra N, Roetzel W. Pool boiling characteristics of nano-fluids. *International Journal of Heat and Mass Transfer*. 2003;**46**(5):851-862
- [29] Jang SP, Lee JH, Hwang KS, Choi SU. Particle concentration and tube size dependence of viscosities of Al<sub>2</sub>O<sub>3</sub>-water nanofluids flowing through micro-and minitubes. *Applied Physics Letters*. 2007;**91**(24):243112
- [30] Timofeeva EV, Gavrilov AN, McCloskey JM, Tolmachev YV, Sprunt S, Lopatina LM, et al. Thermal conductivity and particle agglomeration in alumina nanofluids: Experiment and theory. *Physical Review E*. 2007;**76**(6): 061203
- [31] Williams W, Buongiorno J, Hu LW. Experimental investigation of turbulent

- convective heat transfer and pressure loss of alumina/water and zirconia/water nanoparticle colloids (nanofluids) in horizontal tubes. *Journal of Heat Transfer*. 2008;**130**(4):042412
- [32] Tavman I, Turgut A, Chirtoc M, Schuchmann HP, Tavman S. Experimental investigation of viscosity and thermal conductivity of suspensions containing nanosized ceramic particles. *Archives of Materials Science and Engineering*. 2008;**34**(2):99-103
- [33] Chandrasekar M, Suresh S, Bose AC. Experimental investigations and theoretical determination of thermal conductivity and viscosity of Al<sub>2</sub>O<sub>3</sub>/water nanofluid. *Experimental Thermal and Fluid Science*. 2010;**34**(2):210-216
- [34] Murshed SS. Simultaneous measurement of thermal conductivity, thermal diffusivity, and specific heat of nanofluids. *Heat Transfer Engineering*. 2012;**33**(8):722-731
- [35] Ahammed N, Asirvatham LG, Wongwises S. Effect of volume concentration and temperature on viscosity and surface tension of graphene–water nanofluid for heat transfer applications. *Journal of Thermal Analysis and Calorimetry*. 2016;**123**(2):1399-1409
- [36] Buckingham E. On physically similar systems; illustrations of the use of dimensional equations. *Physical Review*. 1914;**4**(4):345
- [37] Chen H, Ding Y, He Y, Tan C. Rheological behaviour of ethylene glycol based titania nanofluids. *Chemical Physics Letters*. 2007;**444**(4–6):333-337
- [38] Hosseini MS, Mohebbi A, Ghader S. Correlation of shear viscosity of nanofluids using the local composition theory. *Chinese Journal of Chemical Engineering*. 2010;**18**(1):102-107
- [39] Masoumi N, Sohrabi N, Behzadmehr A. A new model for calculating the effective viscosity of nanofluids. *Journal of Physics D: Applied Physics*. 2009;**42**(5):055501
- [40] Vakili-Nezhaad GR, Al-Wadhahi M, Gujarathi AM, Al-Maamari R, Mohammadi M. Molecular dynamics simulation of water–graphene nanofluid. *SN Applied Sciences*. 2019;**1**(3):214
- [41] Vakili-Nezhaad G, Al-Wadhahi M, Gujarathi AM, Al-Maamari R, Mohammadi M. Effect of temperature and diameter of narrow single-walled carbon nanotubes on the viscosity of nanofluid: A molecular dynamics study. *Fluid Phase Equilibria*. 2017;**434**: 193-199